

1-2010

Revealing Linear Aggregates Of Light Harvesting Antenna Proteins In Photosynthetic Membranes

Yufan He

Xiaohua Zeng


Saptarshi Mukherjee

Suneth Rajapaksha

Samuel Kaplan

See next page for additional authors

Follow this and additional works at: https://scholarworks.bgsu.edu/chem_pub

 Part of the [Chemistry Commons](#)

Repository Citation

He, Yufan; Zeng, Xiaohua; Mukherjee, Saptarshi; Rajapaksha, Suneth; Kaplan, Samuel; and Lu, H. Peter, "Revealing Linear Aggregates Of Light Harvesting Antenna Proteins In Photosynthetic Membranes" (2010). *Chemistry Faculty Publications*. 96.
https://scholarworks.bgsu.edu/chem_pub/96

This Article is brought to you for free and open access by the Chemistry at ScholarWorks@BGSU. It has been accepted for inclusion in Chemistry Faculty Publications by an authorized administrator of ScholarWorks@BGSU.

Author(s)

Yufan He, Xiaohua Zeng, Saptarshi Mukherjee, Suneth Rajapaksha, Samuel Kaplan, and H. Peter Lu

Revealing Linear Aggregates of Light Harvesting Antenna Proteins in Photosynthetic Membranes

Yufan He,[†] Xiaohua Zeng,[‡] Saptarshi Mukherjee,[†] Suneth Rajapaksha,[†] Samuel Kaplan,[‡] and H. Peter Lu^{*†}[†]Bowling Green State University, Department of Chemistry, Center for Photochemical Sciences, Bowling Green, Ohio 43403, and [‡]Department of Microbiology and Molecular Genetics, The University of Texas Health Science Center, Medical School, 6431 Fannin, Houston, Texas 77030

Received April 6, 2009. Revised Manuscript Received May 13, 2009

How light energy is harvested in a natural photosynthetic membrane through energy transfer is closely related to the stoichiometry and arrangement of light harvesting antenna proteins in the membrane. The specific photosynthetic architecture facilitates a rapid and efficient energy transfer among the light harvesting proteins (LH2 and LH1) and to the reaction center. Here we report the identification of linear aggregates of light harvesting proteins, LH2, in the photosynthetic membranes under ambient conditions by using atomic force microscopy (AFM) imaging and spectroscopic analysis. Our results suggest that the light harvesting protein, LH2, can exist as linear aggregates of 4 ± 2 proteins in the photosynthetic membranes and that the protein distributions are highly heterogeneous. In the photosynthetic membranes examined in our measurements, the ratio of the aggregated to the nonaggregated LH2 proteins is about 3:1 to 5:1 depending on the intensity of the illumination used during sample incubation and on the bacterial species. AFM images further identify that the LH2 proteins in the linear aggregates are monotonically tilted at an angle $4 \pm 2^\circ$ from the plane of the photosynthetic membranes. The aggregates result in red-shifted absorption and emission spectra that are measured using various mutant membranes, including an LH2 knockout, LH1 knockout, and LH2 at different population densities. Measuring the fluorescence lifetimes of purified LH2 and LH2 in membranes, we have observed that the LH2 proteins in membranes exhibit biexponential lifetime decays whereas the purified LH2 proteins gave single exponential lifetime decays. We attribute that the two lifetime components originate from the existence of both aggregated and nonaggregated LH2 proteins in the photosynthetic membranes.

Introduction

Light-harvesting proteins in photosynthetic membranes play a critical role in converting solar energy to chemical energy through efficient energy transfer processes in purple bacteria.^{1–6} There are primarily two types of light-harvesting proteins, light harvesting complex I (LH1) and light harvesting complex II (LH2), that exist in the membrane. In a conventional model, multiple LH2 complexes peripherally surround the LH1 in a two-dimensional architecture.^{4–9} The initial event in photosynthesis is the photon excitation of LH2, followed by energy transfer among LH2 proteins (LH2 \rightarrow LH2), followed by energy transfer from LH2 to LH1 proteins

(LH2 \rightarrow LH1), which is subsequently funneled to the reaction center (LH1 \rightarrow RC) where a charge separation takes place.^{6,10–16}

Studies on the static protein structures,^{6,17–23} static protein assembly architectures in the membranes,^{22–33} and intramolecular^{11,12,34,35} and intermolecular^{13,14} energy transfer dynamics have

*Corresponding author. E-mail: hplu@bgsu.edu.

- (1) Cogdell, R. J.; Gall, A.; Kohler, J. *Q. Rev. Biophys.* **2006**, *39*(3), 227–324.
- (2) Fleming, G. R.; vanGrondelle, R. *Curr. Opin. Struct. Biol.* **1997**, *7*(5), 738–748.
- (3) Parson, W. W. *Photosynth. Res.* **2003**, *76*(1–3), 81–92.
- (4) Hu, X. C.; Ritz, T.; Damjanovic, A.; Autenrieth, F.; Schulten, K. *Q. Rev. Biophys.* **2002**, *35*(1), 1–62.
- (5) Hu, X. C.; Damjanovic, A.; Ritz, T.; Schulten, K. *Proc. Natl. Acad. Sci. U.S.A.* **1998**, *95*(11), 5935–5941.
- (6) McDermott, G.; Prince, S. M.; Freer, A. A.; Hawthornthwaitelawless, A. M.; Papiz, M. Z.; Cogdell, R. J.; Isaacs, N. W. *Nature* **1995**, *374*(6522), 517–521.
- (7) Miller, K. R. *Nature* **1982**, *300*(5887), 53–55.
- (8) Papiz, M. Z.; Prince, S. M.; Hawthornthwaitelawless, A. M.; McDermott, G.; Freer, A. A.; Isaacs, N. W.; Cogdell, R. J. *Trends Plant Sci.* **1996**, *1*(6), 198–206.
- (9) Monger, T. G.; Parson, W. P. *Biochim. Biophys. Acta* **1977**, *460*, 393–407.
- (10) Brixner, T.; Stenger, J.; Vaswani, H. M.; Cho, M.; Blankenship, R. E.; Fleming, G. R. *Nature* **2005**, *434*(7033), 625–628.
- (11) Sundstrom, V.; Pullerits, T.; van Grondelle, R. J. *Phys. Chem. B* **1999**, *103*(13), 2327–2346.
- (12) Cheng, Y. C.; Silbey, R. J. *Phys. Rev. Lett.* **2006**, *96*(2), 028103.
- (13) Nagarajan, V.; Parson, W. W. *Biochemistry* **1997**, *36*(8), 2300–2306.
- (14) Pan, D.; Hu, D. H.; Liu, R. C.; Zeng, X. H.; Kaplan, S.; Lu, H. P. *J. Phys. Chem. C* **2007**, *111*(25), 8948–8956.
- (15) van Oijen, A. M.; Ketelaars, M.; Kohler, J.; Aartsma, T. J.; Schmidt, J. *Science* **1999**, *285*(5426), 400–402.
- (16) Walla, P. J.; Yom, J.; Krueger, B. P.; Fleming, G. R. *J. Phys. Chem. B* **2000**, *104*(19), 4799–4806.

(17) Allen, J. P.; Feher, G.; Yeates, T. O.; Komiyama, H.; Rees, D. C. *Proc. Natl. Acad. Sci. U.S.A.* **1987**, *84*(17), 6162–6166.

(18) Deisenhofer, J.; Epp, O.; Miki, K.; Huber, R.; Michel, H. *Nature* **1985**, *318*(6047), 618–624.

(19) Roszak, A. W.; Howard, T. D.; Southall, J.; Gardiner, A. T.; Law, C. J.; Isaacs, N. W.; Cogdell, R. J. *Science* **2003**, *302*(5652), 1969–1972.

(20) Bahatryova, S.; Frese, R. N.; van der Werf, K. O.; Otto, C.; Hunter, C. N.; Olsen, J. D. *J. Biol. Chem.* **2004**, *279*(20), 21327–21333.

(21) Fotiadis, D.; Qian, P.; Philippsen, A.; Bullough, P. A.; Engel, A.; Hunter, C. N. *J. Biol. Chem.* **2004**, *279*(3), 2063–2068.

(22) Siebert, C. A.; Qian, P.; Fotiadis, D.; Engel, A.; Hunter, C. N.; Bullough, P. A. *Embo J.* **2004**, *23*(4), 690–700.

(23) Scheuring, S.; Seguin, J.; Marco, S.; Levy, D.; Breyton, C.; Robert, B.; Rigaud, J. L. *J. Mol. Biol.* **2003**, *325*(3), 569–580.

(24) Bahatryova, S.; Frese, R. N.; Siebert, C. A.; Olsen, J. D.; van der Werf, K. O.; van Grondelle, R.; Niederman, R. A.; Bullough, P. A.; Otto, C.; Hunter, C. N. *Nature* **2004**, *430*(7003), 1058–1062.

(25) Frese, R. N.; Olsen, J. D.; Brannvall, R.; Westerhuis, W. H. J.; Hunter, C. N.; van Grondelle, R. *Proc. Natl. Acad. Sci. U.S.A.* **2000**, *97*(10), 5197–5202.

(26) Jamieson, S. J.; Wang, P. Y.; Qian, P.; Kirkland, J. Y.; Conroy, M. J.; Hunter, C. N.; Bullough, P. A. *Embo J.* **2002**, *21*(15), 3927–3935.

(27) Sener, M. K.; Olsen, J. D.; Hunter, C. N.; Schulten, K. *Proc. Natl. Acad. Sci. U.S.A.* **2007**, *104*(40), 15723–15728.

(28) Walz, T.; Jamieson, S. J.; Bowers, C. M.; Bullough, P. A.; Hunter, C. N. *J. Mol. Biol.* **1998**, *282*(4), 833–845.

(29) Scheuring, S.; Busselez, J.; Levy, D. *J. Biol. Chem.* **2005**, *280*(2), 1426–1431.

(30) Scheuring, S.; Goncalves, R. P.; Prima, V.; Sturgis, J. N. *J. Mol. Biol.* **2006**, *358*(1), 83–96.

(31) Scheuring, S.; Rigaud, J. L.; Sturgis, J. N. *Embo J.* **2004**, *23*(21), 4127–4133.

(32) Scheuring, S.; Sturgis, J. N. *Science* **2005**, *309*(5733), 484–487.

(33) Scheuring, S.; Sturgis, J. N.; Prima, V.; Bernadac, A.; Levy, D.; Rigaud, J. L. *Proc. Natl. Acad. Sci. U.S.A.* **2004**, *101*(31), 11293–11297.

(34) Lee, H.; Cheng, Y. C.; Fleming, G. R. *Science* **2007**, *316*(5830), 1462–1465.

(35) Rutkauskas, D.; Cogdell, R. J.; van Grondelle, R. *Biochemistry* **2006**, *45*(4), 1082–1086.

provided extensive knowledge about photosynthetic processes. The intraprotein photosynthetic apparatus structures,^{6,17–23} ultrafast energy transfer among the excitonically coupled chromophores within LH1 and LH2 proteins,^{11,34,35} and even the single-molecule spectroscopy of individual LH2 proteins^{15,35,36} have been extensively studied. However, the nature of interprotein architecture and energy transfer coupling in the photosynthetic membranes is still not clearly understood due to the inhomogeneous distribution of the LH2 and LH1 proteins, complex interactions among the proteins, and dynamic structure fluctuations of the membrane architecture.

Atomic force microscopy (AFM) topographic imaging studies have shown that photosynthetic membranes feature inhomogeneous LH1–LH2 distributions.^{22–25,27–33} Both disordered domains and paracrystalline domains of LH2 proteins in photosynthetic membranes have been observed by AFM imaging.^{22–25,27–33} AFM imaging analysis also identified that the light harvesting proteins may form different architectures under different sample incubation conditions, which reflects the stoichiometric and density differences of LH2 and LH1 in the membranes grown under different light intensities, and buffer conditions, or from different bacterial sources.^{22–24,27,30–32} For example, LH1 proteins were observed to form dimers²⁴ and LH2 proteins were observed to form clusters in the membranes.³¹ Both stripe and circular LH2 architectures have been proposed for LH2 coupling to LH1 in the membranes.^{8,25,37–39} Optical spectroscopy and imaging has also shed light on the interprotein structural arrangements and energy transfer processes, indicating that LH2 aggregation with strong energy transfer coupling may be a dominated formation in the membranes.^{13,14,40,41}

LH2 proteins serve as light harvesting antenna, and the characteristics of LH2 protein networks is critical for understanding the light harvesting nature of the photosynthetic membranes. Here, we report that the spatially and optically coupled linear aggregates of LH2 proteins dominate the protein architecture of the photosynthetic membranes from various bacterial species. Using AFM, optical spectroscopy, confocal microscopy imaging, and lifetime measurements, we provide detailed and critical topographic and spectroscopic characterizations of the linear aggregates in terms of their geometry, arrangement, stoichiometry, and energetic coupling in the photosynthetic membranes under ambient conditions. Our analyses also show that there are aggregated and nonaggregated states of LH2 complex proteins in a 3:1 to 5:1 ratio in the membranes.

Materials and Methods

(a) Bacterial Growth and Sample Preparation. *Rhodobacter sphaeroides* (Strain 2.4.1 and ATCC17025) and *Rhodospirillum rubrum* bacteria samples were grown photosynthetically at a light intensity of 10–20 W/m² (low light intensity) or 100 W/m² (high light intensity) with purging in a gas mixture of 95% N₂ and 5% CO₂. The bacterial cells were harvested at 0.5 O.D. at 600-nm absorption ($A_{600\text{ nm}}$). Membrane fragment vesicles were separated on a sepharose 2B column (50 × 2.0 cm) and were further purified by rate-zonal sucrose gradient centrifugation at 63 500 × g for

10 h. Membranes were isolated following ultracentrifugation at 260 000 × g for 1.0 h. The isolated membranes were then dissolved in 20 mM Tris-HCl at pH 8.0 containing 100 mM NaCl and 1% lauryl *N,N*-dimethylamine-*N*-oxide (LDAO) for the isolation of spectral complexes by DEAE-52 cellulose chromatography and 20–40% sucrose gradient centrifugation at 260 000 × g for 16 h at 4 °C. Purified membrane fragment vesicles and LH2 complexes were stored at –80 °C.

(b) Sample Preparation for AFM Imaging. The photosynthetic membrane fragment sample was adsorbed on a freshly cleaved mica surface (Ted Pella, Redding, CA). For a sample preparation, 25 mM MgCl₂ solution was first used to rinse the mica surface to change the surface charge from negative to positive, which ensured a firm attachment of the membranes on a mica surface. A small drop of adsorption buffer (10 mM Tris-HCl pH 7.5, 150 mM KCl, 25 mM MgCl₂) was then applied to the mica surface, and 2 μL of membrane solution was injected into the drop of the adsorption buffer. After 1–1.5 h incubation, the sample was gently rinsed with buffer (10 mM Tris-HCl pH 7.5, 150 mM KCl) to remove possible multilayer membrane patches which ensured that only single layer membrane fragments were attached to the mica surface. This technique is effective because the interactions between the Mg²⁺-treated mica surface and the proteins in a photosynthetic membrane are stronger than the interactions among the patches of the membranes. Therefore rinsing only removes the multilayer patches but not perturb the protein arrangement in the membrane adsorbed on mica.

(c) Atomic Force Microscopy Imaging. Tapping-mode AFM imaging was performed with a closed-loop multipurpose AFM Scanner (Agilent 5500 SPM Microscope; Agilent Technologies) and an ultrasharp AFM silicon tip (MicroMash) having a spring constant of 0.6 N m⁻¹ and a resonant frequency of ~75 kHz. An image of 512 × 512 pixels² was typically recorded at a line scanning frequency of 1–2 Hz. In the imaging procedure, we ensured that the AFM imaging scanning operation did not modify the topographic features of the membranes by comparing the unchanged topographic features from consecutive images for the same fragment and same imaging area. AFM imaging is able to identify a folded membrane fragment or a stacked membrane fragment from a flat fragment on a mica surface.

The lateral resolution of our AFM imaging is ~1 nm. For a flat sample, such as membranes on mica, under ambient conditions a typical high resolution image can resolve even the details of the LH2 protein structure.^{22–25,27–33} Therefore, we have focused our AFM imaging analysis only on the flat membranes.

(d) Confocal Fluorescence Microscopy. The membrane single-fragment fluorescence spectra and images were acquired with an inverted confocal microscope (Axiovert-200, Zeiss). The sample was excited by a tunable Ti:sapphire laser system (Coherent, MIRA 900) producing 795 nm, 100 fs pulses at a repetition rate of 76 MHz, and the average incident laser power was typically 3–4 μW. The excitation laser light was reflected by a dichroic beam splitter (815 dclp, Chroma Technology) and focused on the sample by a high numerical aperture objective (1.3 NA, 63×, oil, Zeiss).

For a microscopic imaging and spectroscopy measurement, a 20 μL sample solution was spread on a microscope coverslip (0.17 mm thickness, Gold Seal cover glass, 18 × 18 mm²). The sample was raster-scanned with respect to the laser focus by using an x–y piezoelectric closed-loop position-scanning stage (H100, Mad City Lab). The fluorescence emission was collected by the same objective and was filtered with an optical long pass filter (HQ825LP, Chroma Technology). For single membrane fragment confocal imaging, the detector used was a Si avalanche photodiode single photon counting module, APD (SPCM-AQR-14, PerkinElmer). A typical fluorescence image was acquired by continuously raster scanning the sample over the laser focus with a scanning speed of 4 ms/pixel, with each image being 100 × 100 pixels².

(36) Bopp, M. A.; Jia, Y. W.; Li, L. Q.; Cogdell, R. J.; Hochstrasser, R. M. *Proc. Natl. Acad. Sci. U.S.A.* **1997**, *94*(20), 10630–10635.

(37) Jungas, C.; Ranck, J. L.; Rigaud, J. L.; Joliot, P.; Vermeglio, A. *Embo J.* **1999**, *18*(3), 534–542.

(38) Law, C. J.; Cogdell, R. J.; Trissl, H. W. *Photosynth. Res.* **1997**, *52*(2), 157–165.

(39) Ritz, T.; Park, S.; Schulten, K. *J. Phys. Chem. B* **2001**, *105*(34), 8259–8267.

(40) Dunn, R. C.; Holtom, G. R.; Mets, L.; Xie, X. S. *J. Phys. Chem.* **1994**, *98*(12), 3094–3098.

(41) Jirsakova, V.; ReissHusson, F.; Ranck, J. L.; Moya, I. *Photosynth. Res.* **1997**, *54*(1), 35–43.

After the locations of the photosynthetic membrane fragments were determined, the piezo stage was positioned to bring these fragments into the laser focus of the objective to record the fluorescence spectra and the lifetime. The lifetimes were collected by another avalanche photodiode single photon counting module (MPD, Micro Photon Devices) at a time resolution of 35 ps. The fluorescence spectra were recorded with a liquid-nitrogen cooled charged couple detector camera (N2-CCD Spec 10: 400BR, Princeton Instruments, Roper Scientific) coupled to a spectrometer (Acton 150, Acton Research). A series of these fluorescence spectra were collected with an integration time of 1 s.

(e) Ensemble-Averaged Spectroscopic Measurements.

For the measurements of the ensemble-averaged absorption and emission spectra, we used a VARIAN Cary 50 Scan UV–visible Spectrophotometer and a Quantamaster NIR Fluorometer (Photon Technology International).

Results and Discussion

Photosynthetic membranes of *Rhodobacter sphaeroides* and *Rhodospirillum fulvum*⁴² were used in our experiments. In a living bacterial cell, the shape of the photosynthetic organelles or membranes vary as either spherical or tubular for different species.^{19,43,44} Typically, the membrane fragments in solution or on untreated glass surfaces form folded particles with curved structures.⁴⁵ However, under our sample preparation conditions, the membrane fragments in solution were spread on freshly cleaved MgCl₂ treated mica surfaces and the folded membrane particles opened up and laid flat on the electrolyte treated mica surfaces. The rinsing procedure using buffer also ensured that only the flat membrane fragments stuck to the mica surface for AFM analysis. Similar sample preparation procedures have been demonstrated for AFM imaging recently.^{22–25,27–33} AFM images show the spatial distribution of the light harvesting proteins in the membranes at single-molecule spatial resolution. From AFM imaging, LH1 and LH2 proteins can be identified by the fact that a LH1 protein has a larger ring diameter (~12 nm) with a nonhollow center compared to a LH2 protein (~7 nm) in the membrane.

Figure 1A shows an AFM image (180 nm × 180 nm) of a membrane from *Rhodobacter sphaeroides* (Strain 2.4.1), where the ring-shaped features are of single-molecule LH2 proteins. It is remarkable that the majority of LH2 proteins are in the form of linear aggregates rather than nonaggregated or aggregated with other configurations. The average number of LH2 proteins in aggregates is 4 ± 2 (Figure 1B). AFM imaging shows that the LH2 proteins in the linear aggregates are closely associated, and that the interstitial distance from edge to edge of the proteins in the aggregates is typically below 1 nm.

To further evaluate LH2 aggregation, we have measured the AFM images of the single membrane fragments that have LH2 protein (*Rhodobacter sphaeroides* strain 2.4.1) populations at different densities: the high LH2 protein population density (HD) and the low LH2 protein population density (LD) photosynthetic membranes.⁴⁶ The HD and LD membranes were prepared under different incubation and growth conditions, specifically, under weak light (10–20 W/m²) and strong light (100 W/m²) illumination, respectively. The LH2 protein density is high when the incident light is weak, and vice versa. For both the LD and HD membranes, mostly (65–75%) of the LH2

proteins remain in the linear aggregated form, although the nonaggregated LH2 proteins (25%–35%) are also present (Figure 1 and 2).

We examined the wild-type photosynthetic membranes from a number of bacterial species, including *Rhodospirillum fulvum* and a different strain of *Rhodobacter sphaeroides* (strain ATCC17025) in addition to *Rhodobacter sphaeroides* (strain 2.4.1) and its mutant. In all imaging measurements we observed similar linear aggregates of LH2 proteins in the membranes and the aggregates were typically short consisting of less than 6–8 LH2 proteins on average (Supporting Information Figure S1–S3).

We conclude that the architectural feature is not due to the sample preparations and an AFM imaging artifact, and that the observed linear aggregation is due to the intrinsic spatial arrangement within the membranes. This attribution is based on the following observations: (1) The LD membrane samples from the strong light preparation show significantly diluted protein distribution density in the membranes; however, the LH2 proteins in the LD membranes still show linear aggregation (Figure 2). The observation that both HD and LD membranes show similar linear aggregation suggests that the aggregation is not due to spatial congestion of the individual LH2 proteins in the membranes. (2) The random orientations of the linear aggregates (Figures 1A and 2A) indicate that the aggregation is not due to rinsing of the sample by the buffer solution. On the basis of our observation, we conclude that the linear aggregation is an intrinsic property of the LH2 proteins in the membranes, and that the aggregation due to the protein–protein interaction is important for the energy transfer in the photosynthetic membranes. Furthermore, the interaction and coupling among the linear aggregates may not be significant since the aggregates show random orientations and spatial separations in the membranes. Although the physical origin of this property requires further investigations, the implication for the developments of artificial solar energy harvesting architectures to mimic the photosynthetic membranes is interesting and significant.

We have further revealed that each LH2 protein in a linear aggregate monotonically tilts at an angle of $4 \pm 2^\circ$ from the plane of the photosynthetic membranes (Figure 3), based on analyzing ~100 linear aggregates. This result provides further evidence that the LH2 in aggregates are strongly conjugated topographically, which is consistent with two-dimensional crystal studies that found LH2 proteins to have been tilted by a small packing angle of 6.2° in the lipid membrane in a two-dimensional crystal.²³ In a native bacterial cell, the photosynthetic membrane curvature may dictate the tilt angles of the LH2 proteins. Also the tilt angles fluctuate with the thermal fluctuation of the membranes.⁴⁵

Our observation of the LH2 linear aggregation in photosynthetic membranes at room temperature suggests that the aggregated LH2 proteins are energetically favored to exist in a two-dimensional environment, such as membranes and surfaces. The existence of the linear aggregates of LH2 proteins in a native photosynthetic membrane enhances the mechanic strength of the membranes, which is supported by the observation that the texture of photosynthetic membrane patches changes from rigid to flexible when the LH2 proteins are removed from the membrane by mutation.²²

It is understandable that the geometry of the LH2 linear aggregates have a significant relevance and consequence to the light harvesting function of the photosynthetic membranes: (1) the close contact distances among the aggregated LH2 proteins can facilitate a high energy transfer efficiency; (2) the architecture of the LH2 protein aggregates is tolerant

(42) Eraso, J. M.; Kaplan, S. *Biochemistry* **2000**, *39*(8), 2052–2062.

(43) Hickman, D. D.; Frenkel, A. W. *J. Cell Biol.* **1965**, *25*, 261–278.

(44) Oelze, J.; Drews, G. *Biochim. Biophys. Acta* **1972**, *265*, 209–239.

(45) Chandler, D. E.; Hsin, J.; Harrison, C. B.; Gumbart, J.; Schulten, K. *Biophys. J.* **2008**, *95*(6), 2822–2836.

(46) Firsow, N. N.; Drews, G. *Arch. Microbiol.* **1977**, *115*, 299–306.

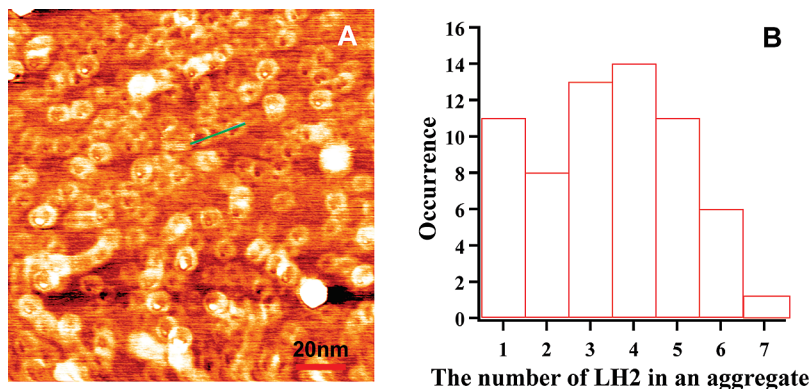


Figure 1. AFM image of light harvesting proteins in photosynthetic membranes. (A) AFM tapping-mode image of light harvesting proteins in a native membrane patch. Majority of the proteins are LH2 and they are mostly in linearly aggregated states. (B) Histogram of LH2 protein linear aggregate length (number of LH2 proteins) in the photosynthetic membrane imaged in A.

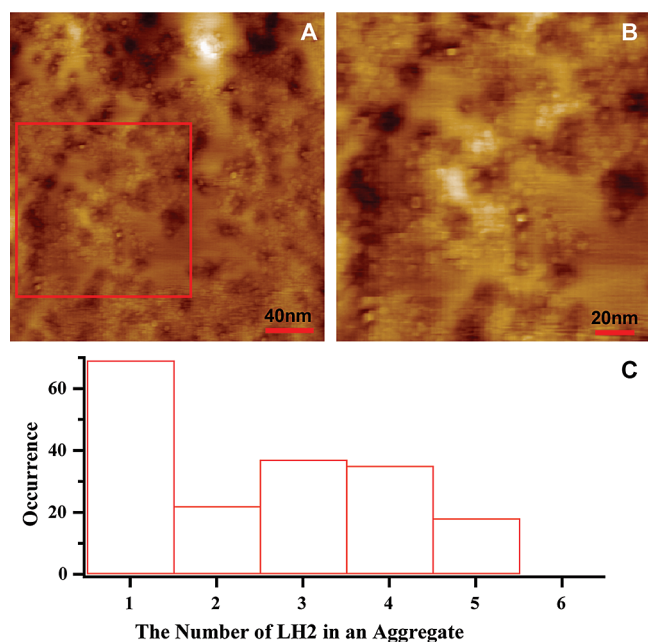


Figure 2. (A) AFM topographic image of a LD membrane sample. The image shows the LH2 proteins still aggregate linearly although the LH2 protein density is lower. (B) Zoom-in from A (area marked). (C) Histogram of LH2 protein linear aggregate length (number of LH2 proteins) in the photosynthetic membrane imaged in A.

to thermal fluctuations within a short linear aggregate; and (3) the finite aggregate length consisting less than 7 proteins in average ensures the efficiency of intermolecular energy transfer but is not susceptible to defects that sink the energy transfer in the photosynthetic membranes.

To further identify the energetic coupling in the LH2 aggregates, we measured the absorption and emission spectra for various photosynthetic membrane fragment samples (Figure 4). The absorption spectrum of the wild-type photosynthetic membranes shows a 2.0 ± 0.2 nm red-shift compared to the absorption of purified LH2 proteins in solution, having an absorption maximum at 850 nm as compared to 848 nm for the purified LH2 proteins (Figure 4A). The emission of a LH1-knockout mutant membrane (lacking LH1) with LH2 proteins shows about a 30-nm red shift at the maximum (895 nm) compared to the maximum emission (866 nm) of the purified LH2 protein in solution (Figure 4B).

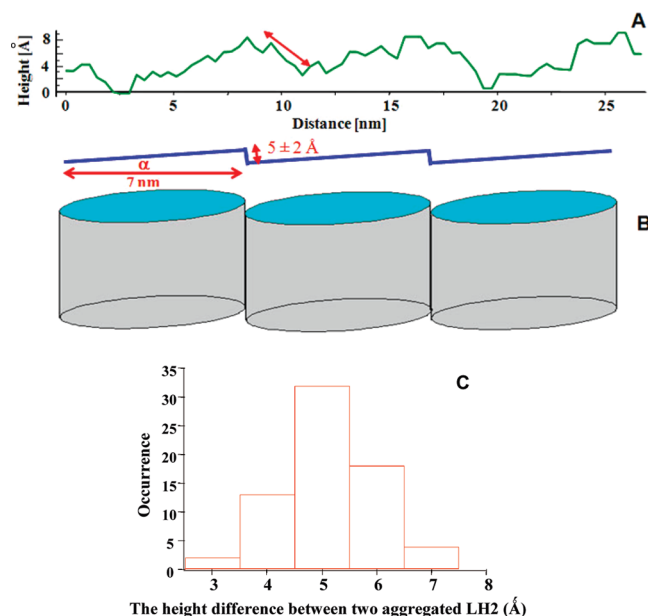


Figure 3. LH2 proteins in a linear aggregate are monotonically tilted at an angle ($4 \pm 2^\circ$) from the membrane surface. (A) Height-amplitude plot along a section line (marked in Figure 1A) from the AFM image in Figure 1A. (B) Model of tilted LH2 in a linear aggregate deduced from A. (C) Histogram of the height difference between two aggregated LH2 molecules.

In a photosynthetic membrane, there is a heterogeneous distribution of aggregated and nonaggregated LH2 proteins having different emission maxima. Figure 4C and 4D show the corresponding emission spectra contributed from both aggregated and nonaggregated LH2 proteins in a membrane. In addition, the absorption spectrum of the membrane LH2 clearly shows a shoulder at 866 nm, which is attributed to the nonaggregated LH2 proteins in the membrane. The red shifts in the absorption and emission suggest that the LH2 protein aggregates in the photosynthetic membranes are energetically coupled. The coupled LH2 aggregates have lower transition energy between the ground state and excited state due to a delocalization of electronic interactions among the aggregated LH2 proteins.

Using AFM imaging, we observed that there are aggregated and nonaggregated two-state LH2 protein assemblies in the photosynthetic membranes, and the ratio of the LH2 proteins in the aggregated states to the nonaggregated states is about 3:1 to 5:1 (Figure 1 and 2). Since the nonaggregated LH2 proteins do not

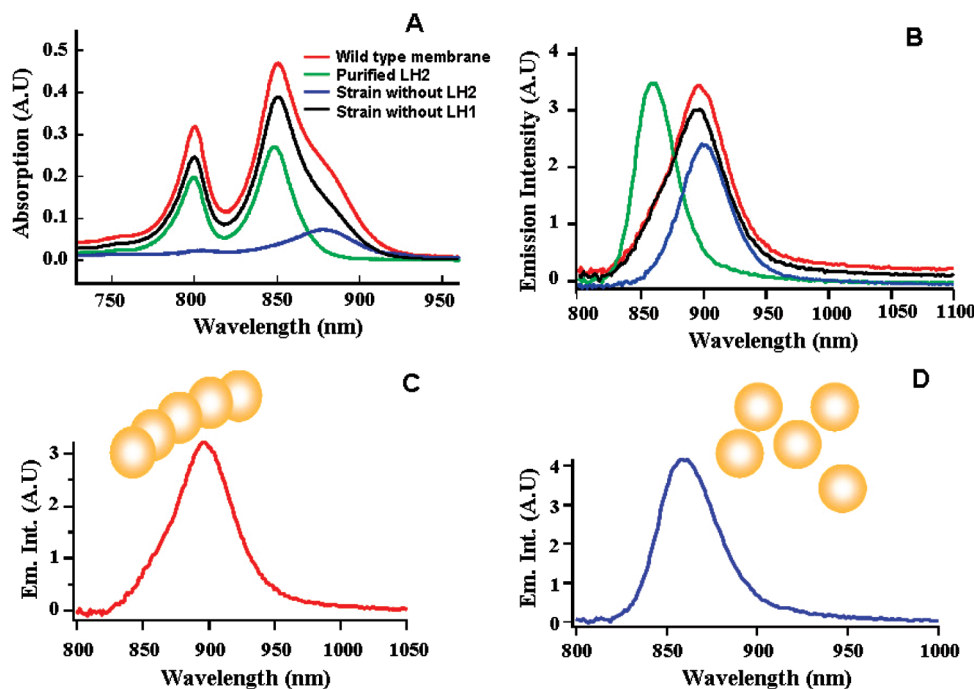


Figure 4. Steady-state absorption and emission spectra of light harvesting proteins and photosynthetic membrane fragments in buffer solution: Purified LH2 proteins in solution (green), mutant membrane with LH2 proteins (LH1 knockout mutation) (black), wild-type membrane (red), and mutant membrane with LH1 proteins (LH2 knockout mutation) (blue). (A) Absorption spectra of samples in buffer solution. (B) Emission spectra of samples in buffer solution. (C and D) Emission spectra of the aggregated LH2 in membranes and purified nonaggregated LH2 proteins in solution.

give red-shifted spectra and the ensemble measured absorption and emission spectra are contributed from the total LH2 proteins including both aggregated and nonaggregated LH2 proteins, the spectral red-shifts for the absorption and emission spectra for the aggregated LH2 proteins should be even larger than what were measured in average over a single membrane fragment (Figure 4). For example, we estimated that the real red shift of the absorption from aggregated LH2 vs nonaggregated LH2 is at least 6 nm.

In a previous publication of a spectroscopy measurement of single wild-type photosynthetic membrane fragments, using two-channel fluorescence resonant energy transfer (FRET) photon-counting detection and a novel two-dimension cross-correlation function amplitude mapping analysis, we have reported observations of significant FRET fluctuations in photosynthetic membranes.¹⁴ We have attributed the FRET fluctuations to the fluctuating energy transfer interaction among LH1–LH2 and LH2–LH2 proteins associated with dynamic coupled and non-coupled states of the light-harvesting protein assemblies in the photosynthetic membranes.¹⁴ The results are intimately related to the dominant existence of the LH2 aggregates in the photosynthetic membranes, that is, the LH2 and LH1 proteins are energetically coupled to a certain degree and environmental thermal fluctuation can significantly perturb the coupling within the LH2 aggregates and couplings between the aggregates and LH1 proteins.

Fluorescence lifetime measurements have been widely used to characterize the light harvesting complexes.^{11,12,34–36,41} It has been reported that nonaggregated LH2 proteins showed single exponential fluorescence decays at a few hundreds of picoseconds to nanoseconds at room temperature.⁴⁷ We found that the fluorescence lifetime decay is biexponential for all of the measured

single photosynthetic membrane fragments, regardless of the population density of the LH2 proteins in the membranes (Figure 5 and 6). We have also observed that the isolated LH2 proteins give single-exponential fluorescence lifetime decays. It is also known that the aggregation of LH2 induces fluorescence quenching and results in the appearance of heterogeneous fluorescence decays with lifetimes in the range of hundreds of picoseconds.^{48,49} The results of our fluorescence lifetime measurements further support the attribution of the existence of both aggregated and nonaggregated LH2 protein populations in the photosynthetic membranes. Our results also suggest that the linear LH2 protein aggregate formation is not due to high population density in the photosynthetic membranes.

Figure 5A shows a fluorescence image of a single HD membrane fragments. The fluorescence lifetime decays measured from the single fragments of the membrane were typically biexponential (Figure 5B–D), which suggests that there exist at least two states of LH2 proteins that give a slow component and a fast component fluorescence lifetime at 325 ± 12 ps and 75 ± 2 ps, respectively. The slower component decays on a similar time scale to that of the nonaggregated LH2 proteins, consistent with the results of our control experiments of isolated LH2 proteins and the lifetimes reported in the literature.^{16,47–49} The faster component can be attributed to the aggregated LH2 proteins in the membrane, being the major component (having pre-exponential factor $\sim 85\%$) of the fluorescence lifetime decay.

The proteins in the membranes exhibits a wide degree of structural and spatial heterogeneity. The temporal heterogeneity is well exemplified in the distributions of the components of the lifetimes as shown in Figure 5C and 5D. The biexponential decay

(48) Mullineaux, C. W.; Pascal, A. A.; Horton, P.; Holzwarth, A. R. *Biochim. Biophys. Acta* **1993**, *1141*(1), 23–28.

(49) van Oort, B.; van Hoek, A.; Ruban, A. V.; van Amerongen, H. *FEBS Lett.* **2007**, *581*(18), 3528–3532.

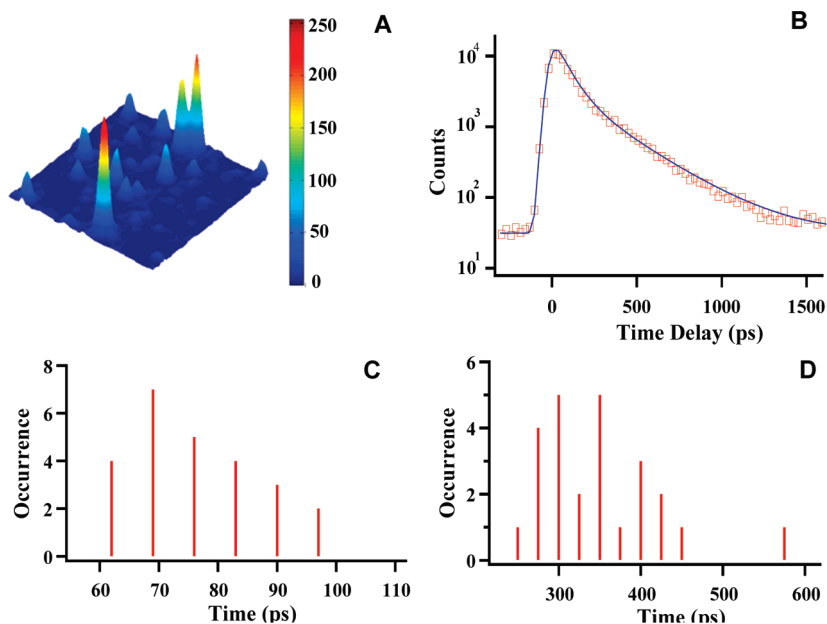


Figure 5. Confocal imaging and lifetime measurements of single high density (HD) LH2 membrane fragments. (A) Fluorescence image ($15 \mu\text{m} \times 15 \mu\text{m}$) of single HD membrane fragments. Each individual peak is attributed to a single LH2 protein fragment and the intensity variation between the fragments is due to the different number of LH2 proteins in the fragments. (B) Fluorescence lifetime measured from a single HD membrane fragment. (C and D) Histograms of the fast component and the slow component from the biexponential fitting of lifetime decays, respectively.

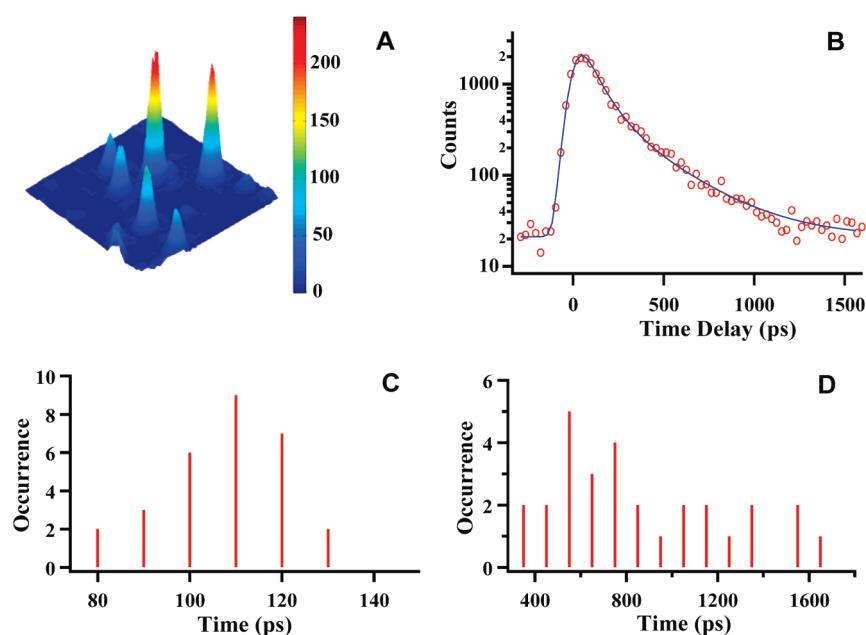


Figure 6. Confocal imaging and lifetime measurements of single low density (LD) LH2 membrane fragments. (A) Fluorescence image ($15 \mu\text{m} \times 15 \mu\text{m}$) of single LD membrane fragments. (B) Fluorescence lifetime measured from a single LD membrane fragment. (C and D) Histograms of the fast component and the slow component from the biexponential fitting of lifetime decays, respectively.

behavior of the fluorescence lifetime remains the same for the LD membrane samples. Figure 6A shows a typical single fragment fluorescence image. The nature of the topographic distributions of the LH2 proteins in the LD membranes as observed by AFM imaging is similar to that observed in the HD membranes having both aggregated and nonaggregated structures. The fluorescence lifetime (Figure 6B) of LD membranes shows similar biexponential decay, and similar distributions (Figure 6C and 6D) of the decay rates with a fast component at 110 ± 10 ps and a slow component in a range from 350 ps to 1.6 ns, which suggests the

existence of at least two states of LH2 proteins in the LD membranes.

The magnitude of the slow component in the LD membranes is significantly different from the HD membranes in terms of the broadness of the distribution, indicating the aggregation states are more inhomogeneous in the LD membranes. For both the HD and LD membrane samples, the aggregated forms of the proteins in the membranes dominate the overall distribution, but the population ratio of aggregation is higher for the HD membranes. In the LD membranes, the probability of observing

nonaggregated single LH2 proteins is higher. This is observable in the AFM topographic images of the LD membranes (Figure 2B) and is reflected in the correlated broad fluorescence lifetime distribution (Figure 6D).

The presence of two states of the aggregated LH2 proteins and nonaggregated LH2 proteins in the membranes from various bacteria species is generally observable by our AFM topographic imaging and spectroscopy measurements. However, significant inhomogeneity existed in the architecture of the membranes, including the density patterns of the distributions, the relative ratio of the aggregated proteins to the nonaggregated proteins, the degree of optical couplings in the aggregated proteins, and the stoichiometry of the aggregations. These parameters relate to the bacteria sample species as well as the sample preparation conditions of light intensity and temperature.

The short linear aggregates of LH2 proteins in the photosynthetic membranes under ambient conditions have a significant similarity to the proposed “stripe” arrangement of the LH1/LH2 proteins^{8,25,37–39} in terms of the topographic features and the fluorescence lifetime reflecting the energy transfer and trapping times. However, our experimental results provide new quantitative details of the overall architecture that is much more inhomogeneous and complex compared to the proposed model architecture. Our observation of short linear aggregates of LH2 proteins in photosynthetic membranes provides important information to help on a comprehensive understanding. Our results are complementary to previously reported light harvesting protein architectural features that exist in the membranes of other species and samples prepared under different conditions.^{3–9,20–35} However, the full implication of the existence of LH2 aggregates in the photosynthetic membranes under ambient conditions for the energy transfer coupling and efficiency in the photosynthetic membranes still needs further systematic investigations.

Conclusion

Our AFM topographic and optical spectroscopic results suggest that both aggregated and nonaggregated LH2 protein assemblies exist in the photosynthetic membranes of high or low protein population densities, and that the distributions are highly heterogeneous in nature. LH2 mostly exist as linear aggregates of 4 ± 2 proteins in the photosynthetic membranes. The LH2 proteins in the linear aggregates are monotonically tilted at an angle $4 \pm 2^\circ$ from the plane of the photosynthetic membranes. Although the tilt angles among LH2 in an aggregate likely fluctuate in a living cell, our observation of the monotonically tilted LH2 in a linear aggregate provides further evidence of a strongly conjugated interaction among the LH2 proteins in the linear aggregate. The ratio of aggregated to nonaggregated LH2 proteins is about 3:1 to 5:1 depending on the intensity of the illumination used during sample incubation and on the bacterial species. The energetic coupling within and among the LH2 aggregates contributes significantly to the light-harvesting efficiency of the photosynthetic membranes. The existence of LH2 aggregates in the photosynthetic membranes under ambient conditions is important for understanding the energy transfer coupling and efficiency in the photosynthetic membranes.

Acknowledgment. H.P.L. acknowledges the support of our research from the National Institute of Environmental Health Sciences of NIH (Grant R01ES017070), from the Office of Science of DARPA (Grant W911NF-06-1-0337), and from the Materials Science Division of the U.S. Army Research office (Grant W911 NF-08-1-0349). S.K. acknowledges the support from NIH (GM15590).

Supporting Information Available: Additional AFM images show linear aggregates of LH2 proteins in the photosynthetic membranes from four different bacteria species. This material is available free of charge via the Internet at <http://pubs.acs.org>.